JACS
JOURNAL OF THE AMERICAN CHEMICAL SOCIETY

Article

pubs.acs.org/JACS

# Controlling Conformations of Conjugated Polymers and Small Molecules: The Role of Nonbonding Interactions

Nicholas E. Jackson,*[,†] Brett M. Savoie,[†] Kevin L. Kohlstedt,[†] Monica Olvera de la Cruz,[†] George C. Schatz,[†] Lin X. Chen,*[,†,‡] and Mark A. Ratner*[,†]

[†]Department of Chemistry, Northwestern University, 2145 Sheridan Road, Evanston, Illinois 60208, United States

[‡]Chemical Sciences and Engineering Division, Argonne National Laboratory, 9700 South Cass Avenue, Argonne, Illinois 60439, United States

Supporting Information

**ABSTRACT:** The chemical variety present in the organic electronics literature has motivated us to investigate potential nonbonding interactions often incorporated into conformational "locking" schemes. We examine a variety of potential interactions, including oxygen−sulfur, nitrogen−sulfur, and fluorine−sulfur, using accurate quantum-chemical wave function methods and noncovalent interaction (NCI) analysis on a selection of high-performing conjugated polymers and small molecules found in the literature. In addition, we evaluate a set of nonbonding interactions occurring between various heterocyclic and pendant atoms taken from a group of representative $\pi$-conjugated molecules. Together with our survey and set of interactions, it is determined that while many nonbonding interactions possess weak binding capabilities, nontraditional hydrogen-bonding interactions, oxygen−hydrogen (CH···O) and nitrogen−hydrogen (CH···N), are alone in inducing conformational control and enhanced planarity along a polymer or small molecule backbone at room temperature.

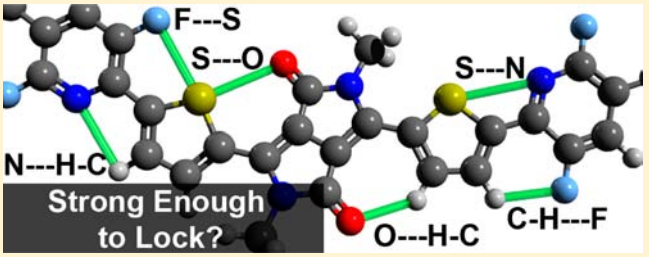


## I. INTRODUCTION

During the past decade, the chemical variety of organic electronics has undergone tremendous growth. The first generation of conducting organic materials witnessed predominantly carbon-based molecular structures such as linear acenes, polyacetylene, and poly(*p*-phenylene vinylene) derivatives (PPV). The following generation involved the widespread incorporation of heterocycles into the conjugated backbone, culminating in the popularization of the thiophene unit as a molecular building block, as in the well-known material poly(3-hexylthiophene), or P3HT. Currently, the standard for high-performing conjugated polymers and small molecules utilizes a so-called "donor−acceptor" design strategy. This method involves synthesizing oligomers and polymers with alternating "electron-rich" and "electron-poor" segments, setting up a local electron density gradient along the backbone, and creating a lower energy charge-transfer transition. The presence of this lower energy transition leads to smaller optical band gaps, larger short-circuit currents, and consequently higher photovoltaic power conversion efficiencies (PCE) when the materials are spin-cast with fullerene acceptors in a bulk heterojunction (BHJ) device.[1,2] This donor−acceptor design strategy has also been linked to many other interesting electronic properties, such as decreased exciton binding energies and ultrafast intramolecular charge transfer.[3,4]

In an attempt to manipulate relevant materials parameters through synthetic expertise, numerous organic heterocyclic and pendant groups have been incorporated into the backbones of donor−acceptor conjugated polymers and small molecules.[2,5] We direct the reader to Figure 1 for a small sampling of the organic functionalities found in the literature that will be featured in this study. When such diverse structural units are incorporated into small molecules and polymers, one creates the possibility for a variety of through-space interactions between different atom

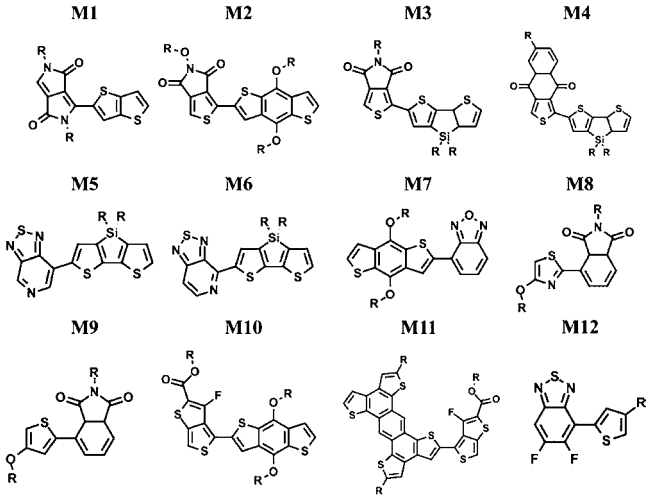


**Figure 1.** The structures featured in this study.[10,11,15−22] These units represent a small sampling of the diverse chemical functionalities present in the donor−acceptor literature. All conformations represent the 0° conformations used throughout this Article.

**Received:** April 12, 2013
**Published:** June 25, 2013

  

types heretofore not commonly noted in previous generations of organic conducting materials. Recently, there has been much speculation on the possibility of weak nonbonding interactions occurring between second and third row elements that are capable of stabilizing particular small molecule or polymer conformations.[6−13] It is clear that in systems as complex as polymers and large oligomers there is a vast conformational space to be explored, and that being able to engineer some degree of control over the inherent disorder through the use of nonbonding interactions is a desirable prospect.

At present, there exists a significant body of work examining the effects of solvent on polymer conformation, polymer conformation on spectroscopic properties, as well as how polymer conformations in the film are inherited from polymer conformations in solution.[14] While insights from these studies are highly useful, they are predominantly qualitative, and have not been performed on donor−acceptor copolymers. Recently, there has been a considerable amount of work in the literature on various synthetic design rules for controlling the conformational distribution in these systems. However, if the crystal structure is unknown (as is generally true for polymers due to polydispersity), then one can infer little absolute knowledge about which conformations are most favorable; even with the crystal structure, one can only speculate as to the mechanisms for conformational preferences, and their relationship to disordered films. With the diverse assortment of organic heterocyclic and pendant groups included in these types of novel materials, and the possible through-space interactions that these engender, determining the most energetically preferable conformation becomes far from intuitive, and understanding the mechanism behind conformational preferences can be difficult.

The goal of this work is to develop a framework for the prediction of conformational preferences based on molecular structure and the diverse nonbonding interactions that result from the chemical variety induced by the popular "donor−acceptor" design strategy. We will achieve this goal through the use of high-level ab initio quantum chemistry, and seek to provide insight to synthetic chemists regarding what interactions are capable of providing conformational control. In addition, we will maintain a firm grounding in previous work, and pay detailed attention to the available crystal structures. Predicting the energetically most stable conformation is a delicate balance of sterics, through-space interactions, degree of $\pi$-conjugation, and a variety of other influences, and this point will be stressed throughout this Article. Last, while the majority of this work focuses on intramolecular interactions, its conclusions should be equally applicable to intermolecular interactions affecting small molecule and polymer films.

## II. COMPUTATIONAL METHODS

To assess the relative conformational energies of donor−acceptor units, it is necessary to examine the torsional potential between two given units. Density functional theory (DFT) has seen widespread use in predicting organic material properties, and has been applied in many cases to determine optimal conformations, as well as inter-ring rotational barriers. While DFT benefits from generally accurate ground-state properties combined with low computational cost, DFT suffers from self-interaction error, which results in an incorrect overdelocalization of the wave function, among other issues.[23,24] Practically speaking, this self-interaction error (SIE) will unfairly bias conformations toward planarity, as a planar conformation will result in the most delocalization of the wave function. In previous studies, this preference for delocalization has manifested itself as artificially large torsional barrier heights and overly planar structures.[25−29] Thus, one must be careful when using DFT, particularly in the case of unconstrained ground-state geometry optimizations, and should question whether the planarity observed is actually an inherent property of the molecule, or an artifact of SIE.

As alternatives to DFT, wave function theories (which do not suffer from SIE) that include pairwise correlation, such as second-order Moller−Plesset perturbation theory (MP2), have been shown to provide reliable barrier heights and relative conformational energies in studies on simple organic molecules.[25,30−32] One inherent downside to electronic structure methods such as MP2 is that they suffer from basis set superposition error (BSSE). However, if one uses a large basis set, these errors can be minimized. MP2 with a sufficiently large basis set (cc-pVTZ) has been proven to provide an accurate representation of long-range dispersion and hydrogen-bonding interactions,[33] another area in which many DFT methods are commonly known to fail (dispersion corrected double-hybrid methods are often an exception).[34,35] In a recent study, it has been concluded that resolution of the identity (RI) MP2 methods with large basis sets is also a reliable means of calculating torsional potentials relevant to conjugated polymers and small molecules, and closely reproduces torsional potentials generated by highly accurate coupled cluster methods.[36]

In this work, we perform computations using resolution of the identity MP2 (RI-MP2), the details of which are provided elsewhere.[37] The RI-MP2 method is known to produce results nearly identical to those of full MP2, and is significantly less expensive computationally.[38] All electronic structure calculations in this work are performed using QCHEM4.0.[39] Comparisons were also made between the RI-MP2 torsional potentials and those obtained from common hybrid DFT (B3LYP/6-31+G**) and empirical force-fields (OPLS2009 force-field[40]). In both cases, potential energy surfaces were found to deviate significantly from calculated RI-MP2/cc-pVTZ surfaces. Consequently, one should not rely upon noncustomized empirical force-fields for the modeling of these materials.

All torsional potentials between adjoining donor and acceptor units are computed at 10° intervals. For each data point, we fix the dihedral angle (specified in the Supporting Information) and perform geometry optimization on all remaining degrees of freedom. These geometry optimizations are performed at the B3LYP/6-31+G** level of theory. In this way, only the nontorsional modes are optimized with DFT. These B3LYP/6-31+G** geometries are then used as the inputs for RI-MP2/cc-pVTZ single-point energy calculations, and the resulting torsional potential energy surfaces are plotted in Figures 2,3, and 4. All side-chains in this study are replaced by methyl groups.

As previous work has postulated the existence of substantial electrostatic interactions between particular second and third row atoms,[6,41] we are interested in computing the partial charges on atoms in particular molecular conformations. We avoid the use of standard Mulliken charges due to their well-known instability with regard to basis set (see the Supporting Information). It is known that far more reliable atomic partial charges can be deduced by fitting the electrostatic potential of the molecule to point charges at each atom in the molecule, under the constraint that the entire molecule remains neutral. We use the "charges from the electrostatic potential on a grid" (ChelpG) method for electrostatic potential fitting implemented in QCHEM 4.0,[42] and fit the electrostatic potential we obtain at the RI-MP2/cc-pVTZ level of theory.

To assess the fundamental strengths of basic atomic through-space interactions, four representative molecules were chosen (Figure 5) that epitomize the fundamental interactions commonly seen along a "donor−acceptor" small molecule or polymer backbone. All individual molecular geometries are initially optimized at the B3LYP/6-311++G** level of theory. The two molecules of interest are then made to lie in the same plane, with the atoms of interest facing each other, and their separation distance is varied. At each chosen separation distance, single-point energy calculations are performed at the RI-MP2/aug-cc-pVTZ level of theory. We choose the slightly larger aug-cc-pVTZ basis set in an attempt to reduce BSSE at small intermolecular distances, which will result in an overbinding of the two molecules. As an additional means of correcting against overbinding, we implement the Boys/Bernardi counterpoise correction[43] to reduce BSSE, where, in addition to the

standard single-point calculation, $E_{AB}^{AB}$, one performs two additional single-point calculations: one with molecule A isolated in a vacuum with its basis functions, as well as the basis functions of "ghost" atoms of molecule B, $E_{A}^{AB}$, and vice versa, $E_{B}^{AB}$. When these energies have been obtained, one then uses eq 1:

$$\Delta E_{int}^{CP}(AB) = E_{AB}^{AB} - E_{A}^{AB} - E_{B}^{AB} \quad (1)$$

to calculate the counterpoise-corrected interaction energy. These interaction energies are then plotted as a function of intermolecular separation (Figure 5), and the binding energy for an interaction is determined by the difference of the energies at the bottom of the potential well, and at a separation where the molecules are no longer interacting. This definition of the binding energy is analogous to that of the Morse potential, and we provide fits to this form in the Supporting Information. We do not calculate the directional dependence of these interactions, but refer to the literature where previous studies[44] have performed in depth analyses of similar directional dependences.

Last, we provide a means for classifying the nonbonding interaction strengths and therefore contribute additional evidence to determine their relevance to conformational locks. Noncovalent interaction (NCI) analysis[45] is performed on M1−M12, for both the 0° and the 180° conformations. NCI is a method that searches for critical points in the electron density topology through the use of the reduced density gradient (RDG). When a singularity in the RDG is found, indicating an electron density critical point, the eigenvalue of the electron density Hessian, along with the magnitude of the density, can be used to determine the strength of a particular nonbonding interaction. Readers may find complete NCI analysis for M1−M12 in the Supporting Information.

## III. RESULTS AND DISCUSSION

**A. Oxygen−Sulfur and Oxygen−Hydrogen Interactions.** Many recent papers have been published regarding a conformational locking "oxygen−sulfur" interaction occurring along donor−acceptor polymer backbones. These interactions have been postulated to occur between thiophene sulfurs and oxygens of both the carbonyl and the ether functionalities. The foundation for this conformational "locking" interaction goes back to a series of studies performed on bithiophene derivatives, where Hartree−Fock calculations and Mulliken partial charge data suggested that there was a large electrostatic interaction between a negatively charged carboxyl oxygen and a positively charged thiophene sulfur, and that this interaction was responsible for the observed crystal structure conformations.[41,46] In numerous other works, it has also been claimed that because the stable conformation of a molecule has the sulfur and oxygen lying within the sum of their respective van der Waals radii, a stabilizing intramolecular interaction is likely occurring.[7,47,48] In other articles, where crystal structures are not present, it has been asserted based on general material properties and DFT geometry optimizations that the small molecules or polymers being studied are highly planar, and are locking into these conformations via through-space oxygen−sulfur interactions.[8−10]

To examine these types of through-space oxygen−sulfur interactions, we have chosen four high-performing donor−acceptor polymers from the literature[13−17,49] with a possible oxygen−sulfur lock akin to those in previous studies (Figure 2). To model the conformational preferences of these polymers, a monomer unit (one donor unit bonded to one acceptor unit) is chosen, and the inter-ring torsional angle is brought through 10° increments, where at each increment a single-point energy calculation is performed, for a total of 180°, as described in the Computational Methods. These results are presented in Figure 2.

From Figure 2, it is clear that for M1, M2, and M3 the 0° conformation with the oxygen−sulfur interaction is energetically unfavorable when compared to the 180° rotated conformation with the oxygen−hydrogen (attached to an aromatic carbon) interaction. In the case of M1, M2, and M3, this relative energy difference is 2.4, 1.6, and 0.8 kcal/mol, respectively. In terms of room-temperature $kT$, these relative energies are 4.1, 2.7, and 1.4 $kT$, respectively. At thermodynamic equilibrium, these would correspond to about 2, 7, and 25 monomers adopting the interacting oxygen−sulfur conformation every 100 units. As these energetic preferences are for the most part noticeably larger than the thermal energy available at room temperature, it appears that there is an influential energetic preference for the conformation that possesses the oxygen−hydrogen interaction over that with the oxygen−sulfur interaction.

It should also be noted that both the 0° and the 180° conformations for M1, M2, and M3 are planar with large rotational barriers, indicating significant electron density present across the inter-ring bond. This is an important fact for studies that have observed material properties suggesting planarity and assigned it to a possible oxygen−sulfur interaction; both the 0° and the 180° conformations are planar and should exhibit material properties indicative of planarity. However, the oxygen−hydrogen interaction conformation is significantly more energetically favorable, and thus is likely the conformation responsible for observed materials properties. We believe that previous computational studies on these interactions would observe the same effect if results were calculated for both the 0° and the 180° conformations of their molecules.[6]

Surprisingly, the conformational preferences of M1, M2, and M3 do not hold true for the case of M4, where the conformation with the oxygen−sulfur interaction is 0.3 kcal/mol more stable than the 180° oxygen−hydrogen conformation; the two conformations are nearly isoenergetic. Additionally, neither minimum in the torsional potential energy surface occurs in a planar conformation, whereas both the 0° and the 180° conformations for M1, M2, and M3 are local minima. These results imply that there are significant unfavorable steric interactions occurring in both the oxygen−sulfur and the oxygen−hydrogen conformations that prevent M4 from being planar. We ascribe this to the inherent geometry differences of the donor and acceptor units. When one looks at the optimized geometries of M1−M4 (see the Supporting Information), one sees that the oxygen−sulfur and oxygen−hydrogen separation distances are significantly smaller (0.3 and 0.1−0.2 Å closer, respectively) for M4 than for M1, M2, and M3. Additionally, the thiophene sulfur−sulfur distance in the 180° conformation is smaller (∼0.15 Å) in M4 than in M1, M2, and M3. From this, it can be concluded that the unfavorable steric interactions occurring in M4 dominate any potential stabilizing oxygen−sulfur interactions. It should also be noticed that the rotational barrier of M4 is significantly smaller than those of M1, M2, and M3, which is indicative of steric interactions raising the relative energies of both potential wells, resulting in the observed reduced rotational barrier height.

Thus, we have arrived at the conclusion that the oxygen−sulfur interaction is not a dominant stabilizing force in our chosen set of materials. Because many of the structural units in M1−M4 are found in high-performing materials throughout the literature, we expect this result to be generally applicable. Intuitively, this conclusion makes sense, as an electronegative oxygen favors a positively charged hydrogen, rather than a sulfur atom, whose electronegativity is similar to that of carbon. One can interpret this energetic preference for the oxygen−hydrogen interaction as a form of hydrogen bonding (CH···OC), given that the oxygen−hydrogen separations, according to B3LYP geometry optimizations, are small (∼2.1−2.2 Å, see the Supporting Information). Such

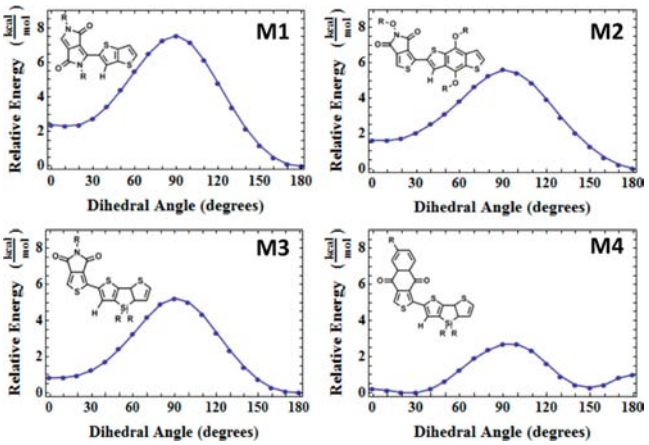


**Figure 2.** Torsional potentials for M1, M2, M3, and M4 calculated at RI-MP2/cc-pVTZ. The molecular conformation shown in each plot is the 0° conformation. Rotation occurs around the inter-ring C−C bond connecting the donor and acceptor blocks.

nontraditional hydrogen-bonding interactions are known to be important throughout the literature.[50−52] These computed distances are far from absolute, but are in agreement with crystal structure results of nearly identical diketopyrrolopyrrole (DPP)-containing small molecules where the intramolecular oxygen−hydrogen distance was determined to be 2.167 Å.[53] Again, it is important to note that sterics play a vital role in determining the relative energies of conformations, and unfavorable sterics can completely overrule potential "locking" mechanisms, as in the case of M4.

These results are slightly controversial, as much previously referenced work has claimed that a stabilizing oxygen−sulfur interaction exists, and is perhaps electrostatic or weakly covalent in nature (a previous analysis assigned the oxygen−sulfur interaction to be van der Waals in nature[29]). Regarding weakly covalent and dispersive interactions, RI-MP2/cc-pVTZ is an accurate level of theory that takes into account pairwise electron correlation and has no reason to fail for our closed-shell organic systems. Therefore, we are confident that we are modeling the majority of important long-range interactions (dipole−dipole dispersion and electrostatics) accurately. If higher-order dispersive interactions were being missed, they would have to result in stabilization on the order of 2 kcal/mol in favor of the oxygen−sulfur conformations to make a significant difference, which is unlikely, as contributions from higher-order multipole interactions should generally be weaker in strength. Regarding the electrostatic mechanism, we analyze the atomic partial charges in our system using the CHelpG electrostatic potential fitting method described in the Computational Methods. These results are presented in Table 1.

**Table 1. Atomic Partial Charges of M1−M4**

| | torsional angle | oxygen charge | sulfur charge | hydrogen charge |
|---|---|---|---|---|
| M1 | 0 | −0.58 | +0.05 | |
| | 180 | −0.65 | | +0.32 |
| M2 | 0 | −0.49 | +0.03 | |
| | 180 | −0.52 | | +0.20 |
| M3 | 0 | −0.53 | +0.07 | |
| | 180 | −0.55 | | +0.19 |
| M4 | 0 | −0.52 | +0.09 | |
| | 180 | −0.57 | | +0.21 |

From Table 1, one observes that no substantial positive charge occurs on the sulfurs of M1−M4. The minor positive charge present on the sulfurs is likely the result of the local polarization of the nearby oxygen atom, and not the inherent chemical structure of the system. This is supported by the fact that the positive charge is largest in M4, which agrees with the fact that the oxygen−sulfur separation distance is smallest for M4, leading to increased polarization from the oxygen. Additionally, it is observed (see the Supporting Information) that the positive charge on the sulfur disappears when the conformation is rotated 180°, supporting the previous conclusion. It is important to note that there is a significant positive charge on the hydrogen, which is consistent with an oxygen−hydrogen bonding interaction, and the greater stability of the oxygen−hydrogen conformation over the oxygen−sulfur conformation. These charge assignments are all in accordance with sulfur having a greater electronegativity than hydrogen, and agree with the general chemistry viewpoint that oxygen−sulfur interactions should be inherently much weaker than oxygen−hydrogen interactions.

As a last note, it is important to compare our computational results to available crystal structures of small molecules in the literature containing similar units. Because of the simple synthetic nature of DPP (M1), many crystal structures can be found in the literature, and all agree with our computed lowest energy oxygen−hydrogen conformation.[53,54] Other synthetic moieties (M2, M3, M4) appearing in small molecule crystal structures with these potential interactions were difficult to find. Crystal structures of fluoranthene-fused imides bonded to thiophenes, containing the common imide group of M2 and M3, show no such locking interaction between oxygen and sulfur occurring in their crystal structures.[55] Additionally, they show no intramolecular oxygen−hydrogen interaction, but do show intermolecular oxygen−hydrogen interactions, which appear to override the intramolecular oxygen−hydrogen interaction. This intermolecular hydrogen-bonding strategy has been utilized in many small molecules.[53,56] Other crystal structure data sets from which this oxygen−sulfur hypothesis began, particularly bithiophene derivatives,[46] cyanothiophene derivatives,[7] and ethylenedioxythiophene (EDOT) derivatives,[47] appear to us to have clear energetically unfavorable steric interactions in the conformation that is not oxygen−sulfur (oxygen−oxygen and oxygen−nitrogen side-chain interactions). We emphasize that simply because a crystal structure shows a conformation with an oxygen−sulfur interaction does not mean that it is the result of that interaction; other larger energy penalties in the system could be minimized by rotating into the oxygen−sulfur interaction, which is not favorable, but is less unfavorable than the alternative (as is the case in M4).

**B. Nitrogen−Sulfur and Nitrogen−Hydrogen Interactions.** In addition to the oxygen−sulfur stabilizing through-space interaction, some researchers have proposed a similar stabilizing nitrogen−sulfur interaction along the polymer backbone.[6,11−13] To assess such interactions, we have chosen four monomers from the literature with possible nitrogen−sulfur, as well as nitrogen−hydrogen, interactions, labeled M5−M8.[10,11,22] Torsional potentials for these donor−acceptor monomer units are presented in Figure 3.

First we compare M5 and M6. These compounds differ only in the position of the nitrogen heteroatom in the pyridine ring. In M5, the nitrogen atom can only influence the torsional potential through conjugative effects, whereas for M6 both steric and through-space interactions are possible. It is clear from Figure 3 that M6 has a significant energetic preference (1.1 kcal/mol) for the 0° conformation bearing a pendant nitrogen−hydrogen interaction. However, the stabilization of the 0° conformation is

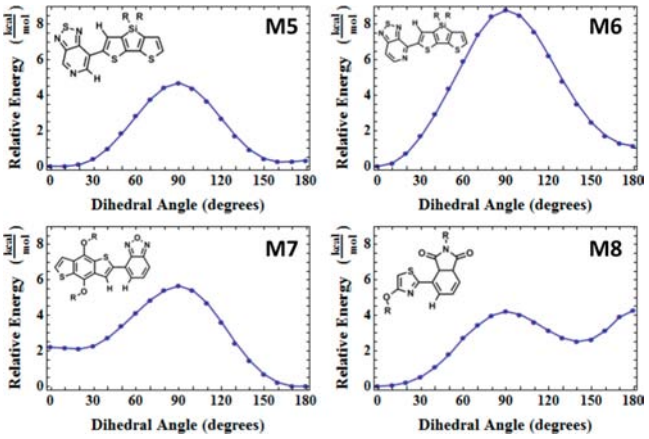


**Figure 3.** Torsional potentials for M5, M6, M7, and M8 calculated at RI-MP2/cc-pVTZ. The molecular conformation shown in each plot is the 0° conformation. Rotation occurs around the inter-ring C−C bond connecting the donor and acceptor blocks.

significantly larger for M6 than for M5 (0.25 kcal/mol), where the hydrogen projecting from the pyridine ring of M5 seems to destabilize both the 0° and the 180° conformations as indicated by the shallow minima and low rotational barrier.

Recently reported crystal structures of M5 and M6[11] suggest that sterics are a determining factor for the observed structure. A decrease in the linearity of the bonded donor and acceptor (increase in the thiadiazole nitrogen to dithienosilole hydrogen distance), described as a banana shape, was observed in M6 as compared to M5. While this result could be ascribed to a nitrogen−sulfur bonding interaction, it is also possible for this effect to be purely steric, as one would expect the replacement of the pyridine C−H (M5) with a nitrogen (M6) to relieve the unfavorable sterics mentioned previously. For this reason, we hesitate to conclude that these results are the consequence of a nitrogen−sulfur interaction.

When one looks at the CHelpG analysis of the M6 0° conformation, with the nitrogen−sulfur interaction present, the nitrogen bears a negative charge of −0.48, and the sulfur a negative charge of −0.02. This fact eliminates any possibility for electrostatic attraction between the two atoms; dispersion interactions may play a role, but as mentioned previously, favorable sterics appear to be the obvious explanation. It should be noted that the thiadiazole nitrogen in the 0° conformation of M5 bears a negative charge of −0.32, and the corresponding hydrogen bears a positive +0.10 charge. Again, this hydrogen-bonding interaction could also be ascribed as a potential reason, in conjunction with favorable sterics, as to why the 0° conformations of M5 and M6 are both more stable than the 180° conformations.

The case of M7 shows characteristics similar to those of M5 and M6. The nitrogen−sulfur conformation is higher in energy than the 180° nitrogen−hydrogen conformation by 2.2 kcal/mol, refuting a potential "locking" interaction. This instability is at least partially due to the hydrogen−hydrogen steric interaction occurring in the 0° conformation, but if such a stabilizing nitrogen−sulfur interaction were present there, it is too weak to relieve this hydrogen−hydrogen steric stress. Instead, the 180° conformation with a nitrogen−hydrogen interaction is significantly more preferable, implying favorable sterics and likely a nitrogen−hydrogen stabilizing interaction, which results in the greatly increased stability of the 180° conformation.

Another point of interest regarding M5 and M6 involves the significantly larger rotational barrier height of M6 as compared to M5. We posit that this is due to the more favorable sterics of M6, which allows the two rings to sit closer together, creating a stronger inter-ring double bond (as manifested in the bond distance of M5 being ∼0.1 Å shorter than that in M6; see the Supporting Information), and thus a higher barrier to rotation. This alone could present a useful design rule for increased planarity in these systems.

M8 (Figure 3) and M9 (Figure 4) represent an ideal case for synthesizing the result of this current section with those of the previous oxygen−sulfur section and are provided for this reason. Both units are identical except that the thiophene 3-carbon in M9 is replaced with a nitrogen atom in M8. In M9, the 0° conformation with the oxygen−sulfur interaction and the hydrogen−hydrogen steric interaction is energetically unfavorable. However, the 180° conformation of M9 sees a significantly lower energy, by 2.0 kcal/mol, where an oxygen−hydrogen interaction is allowed, and the hydrogen−hydrogen steric interaction is replaced by a sterically less problematic sulfur−hydrogen interaction. These results are in agreement with the conclusions of section III.A. It should be noted that in polymers of these units, additional steric congestion is possible that may further disrupt planarity of the backbone.

When one makes the very simple nitrogen substitution to go from M9 to M8, there is a shocking reversal in the relative stability of conformations, and now the 0° conformation is nearly 3 kcal/mol more stable than the 180° conformation. We attribute this to a combination of three effects: (1) the elimination of the unfavorable hydrogen−hydrogen interaction, (2) the more favorable nitrogen−hydrogen interaction (N = −0.32 charge, H = +0.16 charge), and (3) as a result of the less sterically hindered nitrogen−hydrogen interaction, the oxygen−sulfur strain can be relieved as the thiophene sulfur can move further away from the carbonyl oxygen. Thus, we see a variety of effects occurring that cause the entire torsional energy landscape to shift drastically, all by the substitution of a single atom.

In this section, we have assessed the possibility of an electrostatic or weakly covalent "locking" nitrogen−sulfur interaction along polymer backbones and found it unlikely. Further, this interaction has not been shown to play a major role in other systems, such as biological and medicinal chemistry, where the potential for this interaction exists.[57] We conclude that the nitrogen−sulfur interaction is not conformationally influential in conjugated polymer and small molecule systems. Other computational results in the literature have used DFT, natural population analysis, and Bader's atoms-in-molecules[58] analysis to show that there is indeed a nonbonding interaction occurring between nitrogen and sulfur in similar systems. We do not refute the existence of some kind of favorable dispersive interaction, but we do find that these interactions are weak and are unlikely to influence conformations of such molecules at room temperature (see section III.D). It should be noted that our results are restricted to organic, conjugated, closed-shell structures, and for completely different systems (inorganic, nonconjugated, open-shell, etc.) the strengths of these fundamental nonbonding interactions could vary.

The results of both this and the previous section suggest that nontraditional hydrogen-bonding interactions are often under-reported as compared to other competitive nonbonding interactions determining the equilibrium geometries of these systems. We note that, like CH···O, CH···N interactions have also appeared previously in the literature.[59] In section III.D, we

evaluate these atom-to-atom attractions explicitly, and find that nitrogen−hydrogen interactions have the potential to exert conformational control. This makes sense in the context of hydrogen-bonding theory, where O···H, N···H, and F···H are the classic examples of strong hydrogen-bonding interactions.

**C. Fluorine−Sulfur and Fluorine−Hydrogen Interactions.** Because in the previous two sections nontraditional hydrogen-bonding interactions for oxygen−hydrogen and nitrogen−hydrogen have been observed to be possible reasons for differences in conformational stability, it is then useful to speculate on the possibility of the third classic example of hydrogen bonding: the fluorine−hydrogen interaction. This is particularly relevant due to the current trend of fluorinating already high-performing polymers. In many cases, fluorination has led to higher-performing photovoltaic devices, and currently many of these polymers are the constituents of the highest performing organic solar cells available. To assess possible fluorine−hydrogen through-space interactions, we have chosen relevant segments and conformations of three of the highest performing fluorinated polymers from the literature, PTB7 (M10),[19] PTAT3 (M11),[20] and PBnDT-DTffBT (M12).[21]

In Figure 4, it can be immediately discerned that the fluorine-containing compounds show overall lower conformational preferences than the systems already studied. In each case, the stabilization of one conformation over another is no greater than 1 kcal/mol, and the torsional barriers are all less than 3 kcal/mol. One observes that for both M10 and M11, which possess nearly identical sterics, the 180° conformation with the fluorine−hydrogen interaction is more stable than the 0° fluorine−sulfur interaction by 0.6 kcal/mol. This makes sense, as there should be little reason for there to be a favorable through-space interaction between fluorine and something as electronegative as sulfur. In the case of M12, there is only a 0.1 kcal/mol preference for the fluorine−hydrogen interaction, and this is likely due to the fact that fluorine−sulfur and nitrogen−sulfur should have similar nonbonding interactions, and nitrogen−hydrogen and fluorine−hydrogen should have similar interactions, all sterics being the same. As a side note, M12 shows no preference for a possible nitrogen−sulfur interaction, corroborating the results of section III.B.

It is important to clarify that some of the monomer units (notably M10 and M11) have asymmetric chemical structures. This is important because asymmetric units will exhibit different torsional potentials depending on the bonding arrangements of adjacent units. Our results suggest that the torsional potentials are dominated by the local interactions (as discussed in section III.D), which allows us to draw conclusions about the general locking potential of various interactions. However, for a given polymer, the interactions arising between all combinations of neighboring asymmetric units must be carefully considered.

While potential fluorine−hydrogen interactions appear to be favorable, it should be noted that the conformational stability gained by taking advantage of this covalently bound fluorine−hydrogen interaction, in all of these cases, is significantly less than that gained by maximizing potential oxygen−hydrogen and nitrogen−hydrogen interactions. This, however, appears to be a common result,[60] as catalogued in an excellent review on fluorine−hydrogen interactions.[61] In that article, the authors determined covalently bound fluorine−hydrogen interactions to be significantly weaker than the corresponding nitrogen−hydrogen and oxygen−hydrogen interactions. They attribute this to covalently bound fluorine's low proton affinity and its inability to participate in intramolecular electron delocalization or intermolecular cooperative effects when bonded to $\pi$-electron systems. Thus, the fact that the weak stabilization observed here is significantly smaller than in the results of previous sections is to be expected. Regarding potential fluorine−sulfur interactions, there is no intuitive reason that one should expect fluorine and sulfur to interact in a fashion that forms a strong conformational lock (results in the literature are sparse and qualitative[62,63]), but we provide these results for thoroughness.

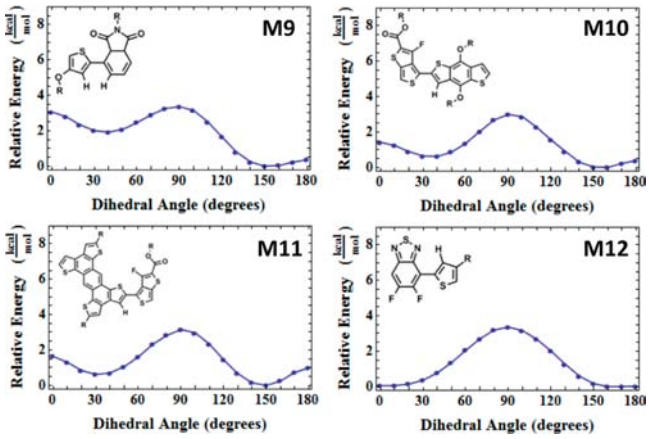


**Figure 4.** Torsional potentials for M9, M10, M11, and M12 calculated at RI-MP2/cc-pVTZ. The molecular conformation shown in each plot is the 0° conformation. Rotation occurs around the inter-ring C−C bond connecting the donor and acceptor blocks.

**D. Analysis of Fundamental Through-Space Interactions.** While the calculations of the previous sections have shown what conformations are preferable based on a combination of sterics and through-space interactions, ultimately one would like to be able to deconvolute the many factors determining stable conformations and simply examine the effect of atom-to-atom nonbonding interactions. In an attempt to achieve this kind of clarity, we have chosen the molecules of Figure 5 as being representative of a variety of possible nonbonding interactions between atoms, which are highlighted. Sulfurs are modeled by the thiophene sulfur, and hydrogens by the thiophene 3-hydrogen. Fluorines are modeled with the fluorine of fluorobenzene, nitrogen with the nitrogen of pyridine, and carbonyl oxygens with the oxygen of acetone. All relevant interactions that could occur along conjugated polymer and small molecule backbones are then calculated as described in the Computational Methods, and binding energies are determined.

From Table 2, it is clear that the dominant interactions are those of nontraditional hydrogen-bonding interactions,

**Table 2. Binding Energies and Equilibrium Distances of Nonbonding Interactions**

| interaction | binding energy (kcal/mol) | equilibrium distance (Å) |
|---|---|---|
| CH−N | 2.20 | ~2.5 |
| CH−O | 1.86 | ~2.4 |
| CH−F | 0.94 | ~2.5 |
| CH−S | 0.74 | ~3.1 |
| S−S | 0.72 | ~4.0 |
| O−S | 0.51 | ~3.4 |
| N−S | 0.46 | ~3.8 |
| F−S | 0.44 | ~3.4 |
| N−F | nonbinding | N/A |
| O−F | nonbinding | N/A |
| O−N | nonbinding | N/A |


dx.doi.org/10.1021/ja403667s | J. Am. Chem. Soc. 2013, 135, 10475−10483

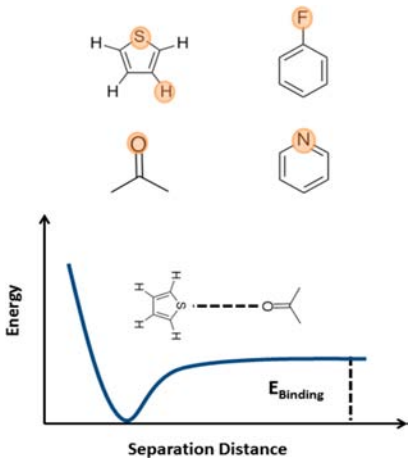


**Figure 5.** Representative molecules used to analyze the strength of nonbonding interactions. Highlighted atoms represent the atoms used in this study. Plot below represents a cartoon of an example calculation (see Supporting Information), where the separation distance of the two atoms is varied, and a potential energy curve is generated. The binding energy of that interaction is defined as the difference between the energy of the molecules at infinite separation and at the minimum of the potential well.

nitrogen−hydrogen and oxygen−hydrogen (nontraditional hydrogen-bonding interactions are weaker than classical hydrogen-bonding interactions, but still influential[50]). These interactions show binding energies of ∼2 kcal/mol (>3 $kT$). Interactions of strength ∼2 $kT$ are generally considered the lower limit for conformational control, as any interaction weaker than that will likely be washed out by thermal fluctuations. To assess if these nontraditional hydrogen-bonding interactions are occurring in the torsional potentials of the materials of sections A, B, and C, NCI analysis is performed on M1−M12 (see the Supporting Information). We find large density basins in the electron density topology, and subsequent critical points are observed for CH···O and CH···N interactions, which we found to be the strongest interactions. The NCI results, while confirming that the nontraditional H-bonds are the strongest interactions, provided a means for enumerating and classifying all of the electrostatic and van der Waals interactions (see Figures S15−S27 in the Supporting Information). To demonstrate the potential efficacy of utilizing intramolecular hydrogen-bonding locks in these systems, we include a relative energy calculation of two conformations of 2,2′-bipyridine (see the Supporting Information) to show that conformational control by maximizing N···H interactions can lead to up to ∼6 kcal/mol differences in stability between cis and trans conformations. Last, we note that the next most influential interaction in Table 2 is the fluorine−hydrogen interaction. While being the third strongest interaction, it is still significantly weaker than the nitrogen and oxygen hydrogen-bonding interactions, in agreement with the conclusions of section C.

It is somewhat surprising to see that many of the potential through-space interactions of Table 2 are capable of forming a bound state (particularly S···O, S···N, S···F). This is in agreement with previous AIM analysis on S···O, S···F, CH···O, and CH···F interactions in bithiophenes.[29] It should be noted that oxygen−sulfur and nitrogen−sulfur are capable of forming very weakly bound states of ∼0.5 kcal/mol (<1 $kT$), which can partially be attributed to the d orbitals of sulfur in these interactions.[64] NCI calculation performed on M1−M12 also confirmed the existence of very weak, but non-negligible interactions of these types (see the Supporting Information). However, in a thermally fluctuating environment at room temperature, as is always the case for small molecules and polymers in organic electronics devices, these interactions are likely insignificant. This is supported from the torsional potentials of sections A, B, and C where we found no evidence that the S···O, S···N, S···F interactions shown in the NCI analysis were capable of influencing conformational preferences.

Certain through-space interactions are, under the assumption of pairwise correlation, entirely unfavorable (deduced by a purely exponential decay of the interaction energy), and thus should not be thought of as the motive for any conformational locking schemes in donor−acceptor type units. Again, we did not suspect there to be significant binding interactions between many of these units (O···F, O···N, N···F), but we provide them for completeness and for the aid of synthetic chemists attempting to build conformational locking mechanisms into new conjugated small molecules and polymers.

Calculations like the ones performed in this section are common in the biological and protein fields,[65,66] where weak noncovalent interactions play a role in determining the minimum energy structures. Such studies generally support the conclusions reached here for conjugated materials; however, direct comparisons are difficult because competing interactions can rarely be deconvoluted in protein systems. Readers interested in a thorough discussion of the directionality and mechanisms for such noncovalent interactions in these systems should consult ref 44. We emphasize that in low temperature crystal structures of biologically relevant molecules, these weak (<0.6 kcal/mol) nonbonding interactions may be of greater importance, but in our highly disordered polymer and small molecule systems at room temperature we doubt they are significant.

Additionally, it is important to note that these calculations have been performed in vacuum, and that solvent effects are not accounted for. In the case of intramolecular interactions, we doubt that solvent molecules are capable of significantly screening these interactions, as the distance between atoms that could undergo nonbonding interactions is generally less than 3 Å, which sterically excludes most solvent molecules used in these systems. However, solvent hydrogen-bonding interactions, while unlikely given the solvents used in these systems (chlorobenzene, chloroform, etc.), could exert significant conformational influences due to chemical variety leading to solvophilic/solvophobic regions. Additionally, solvent could have a noticeable effect screening intermolecular interactions between distinct molecules or polymer chains. We note that screening of nonbonding interactions will only increase the importance of the strongest nonbonding interactions, as weaker interactions will be completely washed out by such screening.

We would like to emphasize that the nonbonding interaction strengths of Table 2 are in good agreement with the conclusions of the torsional potentials considered in sections A, B, and C, as well as the NCI analysis. This reinforces the fact that large contributions to the stability of a given conformation can be determined by only considering local nonbonding interactions. The extent to which these local interactions might propagate along the backbone and determine extended polymer conformation is a highly interesting topic, but is beyond the scope of this work.

A last point involves the commonly made assertion that because two atoms lie at a separation distance that is less than the sum of their respective van der Waals radii, there must be a stabilizing intramolecular interaction occurring to keep them there.[47] While Table 2 suggests that this might be true at some optimal distance, generally speaking, if two atoms are present at a distance below their optimal separation distance, a repulsive


dx.doi.org/10.1021/ja403667s | J. Am. Chem. Soc. 2013, 135, 10475−10483

interaction will occur, as supported by the Morse potential shape of our RI-MP2/aug-cc-pVTZ potential energy curves. Also, while the equilibrium distances presented in Table 2 (rounded to the nearest 0.1 Å) are generally within 0.1−0.2 Å of those that would be determined from the sum of Bondi's van der Waals radii,[67] some significant deviations occur, and the sign of the deviation is not uniform. This calls into question the utility of strict structural characterization using classical Bondi van der Waals radii; while they are highly useful as an approximate tool, quantitative assignment using these distances should be carefully considered, as the optimal distances could deviate meaningfully depending on the nature of the chemical structure. Thus, if one observes two atoms in a crystal structure present next to each other at below the sum of their respective classical van der Waals radii, we encourage researchers to examine other degrees of freedom in their systems that might influence the given conformation, as the use of classical van der Waals radii is not guaranteed to yield a quantitative description of optimal nonbonding distances.

## IV. CONCLUSIONS

In this Article, we have examined the possible intramolecular interactions that occur along high-performing conjugated polymer and small molecule backbones and found that nontraditional hydrogen-bonding interactions play an important role in stabilizing molecular conformations. The covalent fluorine−hydrogen interaction is capable of providing weak stability, but ultimately is much weaker than the corresponding CH···O and CH···N interactions, which show great potential for being used as potential "locking" mechanisms in small molecules and polymers. We find this result to be novel, as such interactions have gone relatively unnoticed in the organic semiconductor literature, and could be potentially useful mechanisms for conformational control and increased backbone planarity. As a result of this, we encourage researchers in the field to examine the role of nontraditional hydrogen-bonding interactions in their systems.

We have also assessed the role of often-referenced oxygen−sulfur and nitrogen−sulfur nonbonding interactions[6−13] and found weak, noninfluential binding tendencies. In addition, we have computed the binding energies of other potential interactions found in the heterocyclic and pendant groups of the donor−acceptor conjugated polymer and small molecule literature. We hope that these will be useful to synthetic polymer chemists looking to design and analyze conformational preferences in their systems using nonbonding interactions, as well as to computational chemists looking to model the energetically most preferable conformations of their materials.

## ■ ASSOCIATED CONTENT

### Supporting Information

Geometries and CHelpG charge analysis of 0° and 180° conformation of M1−M12. Through-space binding potentials (counterpoise-corrected) of representative molecules and fits to Morse potentials. 2,2′-Bipyridine calculations. Geometries of representative molecules used in bonding potential calculations. Mullkien versus CHelpG charge analysis. Comparison of RI-MP2, B3LYP, and OPLS2009 torsional potentials. Absolute energies of all geometry optimized molecules. Noncovalent interaction analysis of M1−M12. This material is available free of charge via the Internet at http://pubs.acs.org.

## ■ AUTHOR INFORMATION

### Corresponding Author

l-chen@northwestern.edu; ratner@northwestern.edu; nicholasjackson2016@u.northwestern.edu

### Notes

The authors declare no competing financial interest.

## ■ ACKNOWLEDGMENTS

We thank the U.S. DOE-BES Argonne-Northwestern Solar Energy Research Center (ANSER), an Energy Frontier Research Center (Award DE-SC0001059), for funding this project. N.E.J. thanks the NSF for the award of a Graduate Research Fellowship (NSF DGE-0824162). B.M.S. thanks the Northwestern U. MRSEC for a predoctoral fellowship. This work was supported by the MRSEC program of the NSF (DMR-1121262) at the Materials Research Center of Northwestern University.

## ■ REFERENCES

(1) Son, H. J.; Carsten, B.; Jung, I. H.; Yu, L. *Energy Environ. Sci.* **2012**, *5*, 8158.
(2) Duan, C.; Huang, F.; Cao, Y. *J. Mater. Chem.* **2012**, *22*, 10416.
(3) Rolczynski, B. S.; Szarko, J. M.; Son, H. J.; Liang, Y.; Yu, L.; Chen, L. X. *J. Am. Chem. Soc.* **2012**, *134*, 4142.
(4) Scarongella, M.; Laktionov, A.; Rothlisberger, U.; Banerji, N. *J. Mater. Chem. C* **2013**, *1*, 2308.
(5) Lin, Y.; Li, Y.; Zhan, X. *Chem. Soc. Rev.* **2012**, *41*, 4245.
(6) Özen, A. S.; Atilgan, C.; Sonmez, G. *J. Phys. Chem. C* **2007**, *111*, 16362.
(7) Hergué, N.; Mallet, C.; Savitha, G.; Allain, M.; Frère, P.; Roncali, J. *Org. Lett.* **2011**, *13*, 1762.
(8) Huang, H.; Chen, Z.; Ortiz, R. P.; Newman, C.; Usta, H.; Lou, S.; Youn, J.; Noh, Y.-Y.; Baeg, K.-J.; Chen, L. X.; Facchetti, A.; Marks, T. *J. Am. Chem. Soc.* **2012**, *134*, 10966.
(9) Guo, X.; Zhou, N.; Lou, S. J.; Hennek, J. W.; Ponce Ortiz, R.; Butler, M. R.; Boudreault, P.-L. T.; Strzalka, J.; Morin, P.-O.; Leclerc, M.; López Navarrete, J. T.; Ratner, M. A.; Chen, L. X.; Chang, R. P. H.; Facchetti, A.; Marks, T. J. *J. Am. Chem. Soc.* **2012**, *134*, 18427.
(10) Guo, X.; Quinn, J.; Chen, Z.; Usta, H.; Zheng, Y.; Xia, Y.; Hennek, J. W.; Ortiz, R. P.; Marks, T. J.; Facchetti, A. *J. Am. Chem. Soc.* **2013**, *135*, 1986.
(11) Welch, G. C.; Bakus, R. C.; Teat, S. J.; Bazan, G. C. *J. Am. Chem. Soc.* **2013**, *135*, 2298.
(12) Welch, G. C.; Perez, L. A.; Hoven, C. V.; Zhang, Y.; Dang, X.-D.; Sharenko, A.; Toney, M. F.; Kramer, E. J.; Nguyen, T.-Q.; Bazan, G. C. *J. Mater. Chem.* **2011**, *21*, 12700.
(13) Tian, Y.-H.; Kertesz, M. *Macromolecules* **2009**, *42*, 2309.
(14) Schwartz, B. J. *Annu. Rev. Phys. Chem.* **2003**, *54*, 141.
(15) Bronstein, H.; Chen, Z.; Ashraf, R. S.; Zhang, W.; Du, J.; Durrant, J. R.; Shakya Tuladhar, P.; Song, K.; Watkins, S. E.; Geerts, Y.; Wienk, M. M.; Janssen, R. A. J.; Anthopoulos, T.; Sirringhaus, H.; Heeney, M.; McCulloch, I. *J. Am. Chem. Soc.* **2011**, *133*, 3272.
(16) Piliego, C.; Holcombe, T. W.; Douglas, J. D.; Woo, C. H.; Beaujuge, P. M.; Fréchet, J. M. J. *J. Am. Chem. Soc.* **2010**, *132*, 7595.
(17) Chu, T.-Y.; Lu, J.; Beaupré, S.; Zhang, Y.; Pouliot, J.-R.; Wakim, S.; Zhou, J.; Leclerc, M.; Li, Z.; Ding, J.; Tao, Y. *J. Am. Chem. Soc.* **2011**, *133*, 4250.
(18) Cui, C.; Fan, X.; Zhang, M.; Zhang, J.; Min, J.; Li, Y. *Chem. Commun.* **2011**, *47*, 11345.
(19) Liang, Y.; Xu, Z.; Xia, J.; Tsai, S.-T.; Wu, Y.; Li, G.; Ray, C.; Yu, L. *Adv. Mater.* **2010**, *22*, E135.
(20) He, F.; Wang, W.; Chen, W.; Xu, T.; Darling, S. B.; Strzalka, J.; Liu, Y.; Yu, L. *J. Am. Chem. Soc.* **2011**, *133*, 3284.
(21) Zhou, H.; Yang, L.; Stuart, A. C.; Price, S. C.; Liu, S.; You, W. *Angew. Chem., Int. Ed.* **2011**, *123*, 3051.
(22) Nie, W.; MacNeill, C. M.; Li, Y.; Noftle, R. E.; Carroll, D. L.; Coffin, R. C. *Macromol. Rapid Commun.* **2011**, *32*, 1163.
(23) Cohen, A. J.; Mori-Sánchez, P.; Yang, W. *Science* **2008**, *321*, 792.
(24) Cohen, A. J.; Mori-Sánchez, P.; Yang, W. *Chem. Rev.* **2011**, *112*, 289.
(25) Kwasniewski, S. P.; Claes, L.; François, J. P.; Deleuze, M. S. *J. Chem. Phys.* **2003**, *118*, 7823.

(26) Choi, C. H.; Kertesz, M.; Karpfen, A. *Chem. Phys. Lett.* **1997**, *276*, 266.
(27) Ho Choi, C.; Kertesz, M.; Karpfen, A. *J. Chem. Phys.* **1997**, *107*, 6712.
(28) Zhao, Y.; Truhlar, D. G. *J. Phys. Chem. B* **2006**, *110*, 10478.
(29) Raos, G.; Famulari, A.; Meille, S. V.; Gallazzi, M. C.; Allegra, G. *J. Phys. Chem. B* **2004**, *108*, 691.
(30) DuBay, K. H.; Hall, M. L.; Hughes, T. F.; Wu, C.; Reichman, D. R.; Friesner, R. A. *J. Chem. Theory Comput.* **2012**, *8*, 4556.
(31) Wang, L.; Berne, B. J.; Friesner, R. A. *Proc. Natl. Acad. Sci. U.S.A.* **2012**, *109*, 1937.
(32) Raos, G.; Famulari, A.; Marcon, V. *Chem. Phys. Lett.* **2003**, *379*, 364.
(33) Riley, K. E.; Platts, J. A.; Řezáč, J.; Hobza, P.; Hill, J. G. *J. Phys. Chem. B* **2012**, *116*, 4159.
(34) Goerigk, L.; Grimme, S. *Phys. Chem. Chem. Phys.* **2011**, *13*, 6670.
(35) Burns, L. A.; Mayagoitia, Á. V.; Sumpter, B. G.; Sherrill, C. D. *J. Chem. Phys.* **2011**, *134*, 084107.
(36) Sears, J. S.; Chance, R. R.; Brédas, J.-L. *J. Am. Chem. Soc.* **2010**, *132*, 13313.
(37) Feyereisen, M.; Fitzgerald, G.; Komornicki, A. *Chem. Phys. Lett.* **1993**, *208*, 359.
(38) Katouda, M.; Nagase, S. *J. Chem. Phys.* **2010**, *133*, 184103.
(39) Shao, Y.; Molnar, L. F.; Jung, Y.; Kussmann, J.; Ochsenfeld, C.; Brown, S. T.; Gilbert, A. T. B.; Slipchenko, L. V.; Levchenko, S. V.; O'Neill, D. P.; R., A. D., Jr.; Lochan, R. C.; Wang, T.; Beran, G. J. O.; Besley, N. A.; Herbert, J. M.; Lin, C. Y.; Voorhis, T. V.; Chien, S. H.; Sodt, A.; Steele, R. P.; Rassolov, V. A.; Maslen, P. E.; Korambath, P. P.; Adamson, R. D.; Austin, B.; Baker, J.; Byrd, E. F. C.; Dachsel, H.; Doerksen, R. J.; Dreuw, A.; Dunietz, B. D.; Dutoi, A. D.; Furlani, T. R.; Gwaltney, S. R.; Heyden, A.; Hirata, S.; Hsu, C.-P.; Kedziora, G.; Khalliulin, R. Z.; Klunzinger, P.; Lee, A. M.; Lee, M. S.; Liang, W.; Lotan, I.; Nair, N.; Peters, B.; Proynov, E. I.; Pieniazek, P. A.; Rhee, Y. M.; Ritchie, J.; Rosta, E.; Sherrill, C. D.; Simmonett, A. C.; Subotnik, J. E.; Iii, H. L. W.; Zhang, W.; Bell, A. T.; Chakraborty, A. K.; Chipman, D. M.; Keil, F. J.; Warshel, A.; Hehre, W. J.; Iii, H. F. S.; Kong, J.; Krylov, A. I.; Gill, P. M. W.; Head-Gordon, M. *Phys. Chem. Chem. Phys.* **2006**, *8*, 3172.
(40) Jorgensen, W. L.; Maxwell, D. S.; Tirado-Rives, J. *J. Am. Chem. Soc.* **1996**, *118*, 11225.
(41) Pomerantz, M.; Cheng, Y. *Tetrahedron Lett.* **1999**, *40*, 3317.
(42) Breneman, C. M.; Wiberg, K. B. *J. Comput. Chem.* **1990**, *11*, 361.
(43) Boys, S. F.; Bernardi, F. *Mol. Phys.* **1970**, *19*, 553.
(44) Iwaoka, M.; Takemoto, S.; Tomoda, S. *J. Am. Chem. Soc.* **2002**, *124*, 10613.
(45) Contreras-García, J.; Johnson, E. R.; Keinan, S.; Chaudret, R.; Piquemal, J.-P.; Beratan, D. N.; Yang, W. *J. Chem. Theory Comput.* **2011**, *7*, 625.
(46) Pomerantz, M.; Amarasekara, A. S.; Dias, H. V. R. *J. Org. Chem.* **2002**, *67*, 6931.
(47) Roncali, J.; Blanchard, P.; Frère, P. *J. Mater. Chem.* **2005**, *15*, 1589.
(48) Irvin, J. A.; Schwendeman, I.; Lee, Y.; Abboud, K. A.; Reynolds, J. R. *J. Polym. Sci., Part A: Polym. Chem.* **2001**, *39*, 2164.
(49) Cui, C.; Fan, X.; Zhang, M.; Zhang, J.; Min, J.; Li, Y. *Chem. Commun.* **2011**, *47*, 11345.
(50) Scheiner, S. *J. Phys. Chem. B* **2005**, *109*, 16132.
(51) Yoshida, H.; Kaneko, I.; Matsuura, H.; Ogawa, Y.; Tasumi, M. *Chem. Phys. Lett.* **1992**, *196*, 601.
(52) Gu, Y.; Kar, T.; Scheiner, S. *J. Am. Chem. Soc.* **1999**, *121*, 9411.
(53) Naik, M. A.; Venkatramaiah, N.; Kanimozhi, C.; Patil, S. *J. Phys. Chem. C* **2012**, *116*, 26128.
(54) Qiao, Y.; Guo, Y.; Yu, C.; Zhang, F.; Xu, W.; Liu, Y.; Zhu, D. *J. Am. Chem. Soc.* **2012**, *134*, 4084.
(55) Zhou, Y.; Ding, L.; Shi, K.; Dai, Y.-Z.; Ai, N.; Wang, J.; Pei, J. *Adv. Mater.* **2012**, *24*, 957.
(56) Głowacki, E. D.; Irimia-Vladu, M.; Kaltenbrunner, M.; Gąsiorowski, J.; White, M. S.; Monkowius, U.; Romanazzi, G.; Suranna, G. P.; Mastrorilli, P.; Sekitani, T.; Bauer, S.; Someya, T.; Torsi, L.; Sariciftci, N. S. *Adv. Mater.* **2012**, *25*, 1563.
(57) Lin, S.; Wrobleski, S. T.; Hynes, J., Jr.; Pitt, S.; Zhang, R.; Fan, Y.; Doweyko, A. M.; Kish, K. F.; Sack, J. S.; Malley, M. F.; Kiefer, S. E.; Newitt, J. A.; McKinnon, M.; Trzaskos, J.; Barrish, J. C.; Dodd, J. H.; Schieven, G. L.; Leftheris, K. *Bioorg. Med. Chem.* **2010**, *20*, 5864.
(58) Bader, R. F. *Atoms in Molecules: A Quantum Theory*; Clarendon Press: Oxford, 1995.
(59) Domagała, M.; Grabowski, S. J. *J. Phys. Chem. B* **2005**, *109*, 5683.
(60) Reichenbächer, K.; Süss, H. I.; Hulliger, J. *Chem. Soc. Rev.* **2005**, *34*, 22.
(61) Dunitz, J. D.; Taylor, R. *Chem.-Eur. J.* **1997**, *3*, 89.
(62) Wang, Y.; Parkin, S. R.; Gierschner, J.; Watson, M. D. *Org. Lett.* **2008**, *10*, 3307.
(63) Subramanian, S.; Park, S. K.; Parkin, S. R.; Podzorov, V.; Jackson, T. N.; Anthony, J. E. *J. Am. Chem. Soc.* **2008**, *130*, 2706.
(64) Angyan, J. G.; Poirier, R. A.; Kucsman, A.; Csizmadia, I. G. *J. Am. Chem. Soc.* **1987**, *109*, 2237.
(65) Jurečka, P.; Šponer, J.; Černý, J.; Hobza, P. *Phys. Chem. Chem. Phys.* **2006**, *8*, 1985.
(66) Mintz, B. J.; Parks, J. M. *J. Phys. Chem. B* **2012**, *116*, 1086.
(67) Bondi, A. *J. Phys. Chem.* **1964**, *68*, 441.